On the Role of Sea Ice and Convection in a Global Ocean Model

ACHIM STÖSSEL AND KUN YANG

Department of Oceanography, Texas A&M University, College Station, Texas

SEONG-JOONG KIM

Canadian Center for Climate Modelling and Analysis, University of Victoria, Victoria, British Columbia, Canada

(Manuscript received 27 June 2000, in final form 29 August 2001)

ABSTRACT

An earlier estimate regarding the possible impact of sea ice on deep-ocean water mass properties and the global thermohaline circulation in a coupled sea ice–ocean general circulation model (OGCM) is updated. Compared to the earlier application, the main upgrade is a subgrid-scale plume-convection parameterization that replaces conventional grid-cell-wide convective adjustment. The different treatment of convection leads to some noticeable differences in some of the repeated sensitivity experiments. For example, in an experiment where sea ice salinity is assumed to be that of the upper ocean, thus neglecting the primary effect of sea ice formation and melting on the ocean's buoyancy forcing, Antarctic Bottom Water formation comes essentially to a halt, the global deep-ocean properties and thermohaline circulation thus being almost solely determined by North Atlantic Deep Water. The much weaker impact in the earlier estimate turns out to be mainly due to excessive open-ocean convection in the Southern Ocean, rendering that region susceptible to the open-ocean polynya mode. The associated melting in such polynyas leads to an enhancement of convection in a salty sea ice experiment, thus obscuring the effect of neglected brine release in coastal polynyas. Besides underscoring the necessity of a careful treatment of sea ice and convection in the Southern Ocean of a global OGCM, this study indicates that new-ice formation around Antarctica has a much larger effect on global deep-ocean properties and circulation than previously estimated.

1. Introduction

As indicated in several recent scientific meetings and papers, there is much uncertainty associated with the question on the role of polar processes in global climate (e.g., Schmidt and Hansen 1999; Allison et al. 2001). One aspect here is the impact of high-latitude surface conditions on the atmospheric circulation. This is mainly determined by the ice-albedo effect (Curry et al. 1995; Rind et al. 1997) and the large heat fluxes over open water within the sea-ice pack (e.g., leads and polynyas) (Andreas and Murphy 1986; Grötzner et al. 1996; Andreas and Cash 1999). Both depend on the texture of the sea ice–ocean admixture, which is normally just given in terms of the percent areal coverage or concentration of sea ice. The large fluxes over leads have their counterpart in the ocean. Over leads, the coupling to the atmosphere is strongest, and mostly associated with intense cooling and new-ice formation. The latter, in turn, yields strong brine rejection that leads to local destabilization of the water column. Especially in the Southern Ocean (SO), this results in entrainment of warmer, deeper water into the mixed layer and possibly deep-penetrating overturning in the case of open-ocean convection (Martinson 1990; Gordon and Huber 1990; Akitomo et al. 1995; Killworth 1983; Paluszkiewicz and Romea 1997; Visbeck et al. 1995; Carmack 1990), or storage of salty water on continental shelves and eventual downslope flow of that water, in the case of near-boundary convection (Gordon 1998; Killworth 1983; Gill 1973; Foster and Carmack 1976; Jacobs et al. 1985; Whitworth et al. 1998; Jiang and Garwood 1995; Orsi et al. 1999). Both processes determine deep- and bottom-water formation. Both open-ocean and alongslope (near boundary) convection is observed in plumes on horizontal scales of the order of 500–1000 m (Marshall and Schott 1999; Baines and Condie 1998; Harvey 1996).

Deep- and bottom-water formation in global ocean general circulation models (OGCMs) will depend critically on the representation of leads and convection, neither of which can be explicitely resolved in such models (including eddy-resolving OGCMs). Both are thus in need of careful subgrid-scale parameterization. The effect of the latter on deep-ocean properties in association with SO sea ice is the main focus of this study.

Corresponding author address: Dr. Achim Stössel, Department of Oceanography, Texas A&M University, College Station, TX 77843-3146.
E-mail: achim@advect.tamu.edu

We believe that a poor model description of the subtle interplay between ice formation and plume convection is one of the key problems that lead to substantial climate drift or misrepresentation of the deep ocean in climate change studies using coupled atmosphere–sea ice–ocean GCMs (e.g., Bryan 1998; Gordon et al. 2000; Khodri et al. 2001; Barnett et al. 2001).

Conventional ''convective adjustment'' allowing for instantaneous removal of vertical instabilities in water columns on horizontal grid scales of the order of 100 km is not adequate, as discussed, for example, in Marshall and Schott (1999) and Goosse and Fichefet (2001). Replacing convective adjustment by the subgrid-scale plume-convection parameterization of Paluszkiewicz and Romea (1997) in their sea ice–ocean GCM, Kim and Stössel (2001, hereafter KS) found several significant global- and regional-scale improvements, such as a substantial warming and salinification of the global-mean deep and bottom waters toward observed estimates, a much more realistic representation of warm and saline Lower Circumpolar Deep Water (LCDW) along the Antarctic continental margin, and a much more realistic thickness and seasonality of SO sea ice. Note that LCDW is one critical ingredient in the Antarctic Bottom Water (AABW) formation process (Gordon 1998, and references therein).

In KS, a main effect of the plume convection scheme was a reduction of open-ocean convection in the SO to almost zero [as observed (e.g., Marshall and Schott 1999) and aimed at in global OGCMs (e.g., Duffy et al. 1997)], while near-boundary convection was maintained. The access of LCDW by open-ocean subgrid plumes in the early part of the ice growth season prompted slow ice growth and the observed seasonal asymmetry in ice volume (Gloersen et al. 1992). With convective adjustment, on the other hand, LCDW was not accessible up until late in the ice growth season. At that stage, the grid-cell-wide overturning led to large upward heat flux and resulted in the open-ocean polynya mode (e.g., Martinson 1990; Marsland and Wolff 2001; Broecker 1999), which was maintained by the positive feedback of buoyancy loss through surface cooling, while new-ice formation was inhibited by the strong oceanic heat flux. This mode resulted in a seasonally much earlier decline of ice volume than observed and an overall underestimate of ice thickness.

Another important factor in capturing the first-order southern high-latitude processes in global OGCMs is wide continental shelves around Antarctica, as discussed in Kim and Stössel (1998). With (realistically) wide shelves, the first-order features of cold and salty high-salinity shelf water (HSSW) (Jacobs and Guilivi 1998; Foldvik et al. 1985) were captured. This water mass constitutes the other major ingredient in the formation process of AABW (Gordon 1998). A further prerequisite for a reasonable representation of the major SO processes in a global OGCM is sea ice driven by winds that include variability on the atmospheric synoptic scale (see, e.g., Stössel et al. 1998, hereafter SKD).

The fact that all three processes mentioned reveal highly sensitive impacts on the deep-ocean water mass properties and circulation prompted us to manifest the findings of SKD by repeating some of their experiments in a more realistic model setup that includes these processes. In addition, the current model version is enhanced by a globally consistent heat balance calculation.

After introducing the model, the major upgrades of the current model version versus SKD will be described. This is followed by a description of the results, first addressing the differences to KS, then investigating the sensitivity of three first-order sea-ice-related effects, under convective adjustment as well as under plume convection, respectively. This is followed by a discussion, then a final summary and conclusions.

2. The model

a. Basic version

This modeling study employs a global dynamic–thermodynamic sea ice–primitive equation ocean GCM with ''real'' topography. It is basically the same model as used in SKD. The ocean component is a regular spherical-grid coarse-resolution version of the Hamburg Ocean Primitive Equation model [for technical details see Wolff et al. (1997)], the basic physics of which are identical to the more widely used Geophysical Fluid Dynamics Laboratory (GFDL) Modular Ocean Model (Pacanowski 1995). The spatial discretization and the grid resolution are the same as in Drijfhout et al. (1996) and Maier-Reimer et al. (1993), using an Arakawa E grid with an effective horizontal resolution of 3.5°, 11 vertical layers with actual topography-following bottom-layer depth (the topography thus being much finer resolved than the vertical resolution would allow), and a prognostic free sea surface. The justification for the coarse grid resolution is to yield a tool that can be used for a series of near-equilibrium sensitivity integrations (see below).

Crucial for our investigation is a comprehensive dynamic–thermodynamic sea ice component. Its dynamic part is based on a viscous–plastic rheology, referring to Hibler (1979), while thermodynamic ice growth and decay are determined by separate heat balance calculations over the subgrid ice-free and ice-covered parts, referring back to Maykut (1986) and Owens and Lemke (1990). Optionally, a prognostic snow cover can be accounted for.

The overall atmospheric forcing fields are also the same as in SKD, namely, the climatologies of Hellerman and Rosenstein (1983) for monthly winds (except over SO sea ice; see below) and of Woodruff et al. (1987) [Comprehensive Ocean–Atmosphere Data Set (COADS)] for monthly air temperatures. In order to mimick the freshwater flux, upper-ocean salinities are

restored to the Levitus (1982) climatology. Additionally, outbreaks of continental air masses, such as frequently observed along mid- and high-latitude east coasts, are accounted for by modifying the COADS air temperature by advection through winds [Eq. (15) in Maier-Reimer et al. 1993].

As in SKD, the current version has a restoring timescale for salinity of 40 days, and there is no salinity restoring under sea ice. Furthermore, the horizontal and vertical diffusion coefficients for heat and salt (D_H and D_V), as well as the horizontal and vertical eddy viscosities (A_H and A_V), are all identical to those in SKD ($D_H = 2 \times 10^3$ m^2 s^{-1}, $D_V = 8 \times 10^{-5}$ m^2 s^{-1}, $A_V = 2 \times 10^{-4}$ m^2 s^{-1}; A_H is grid-size dependent, the maximum thus occurring at the equator where it reads 2×10^5 m^2 s^{-1}). This model has no isopycnal mixing parameterization.

b. Upgrades

In comparison to SKD, four major improvements toward a more realistic model representation of high-latitude processes have been considered for this study.

1) The continental shelves around Antarctica have been widened toward a more realistic bathymetry. The positive effect of this measure has been discussed in Kim and Stössel (1998) (see also section 1).

2) The surface heat-balance calculation as used in SKD over grid cells that contain sea ice is now used globally. This replaces the plain temperature restoring beyond SO sea ice and has been pursued in order to attain a globally consistent surface heat-flux calculation. While this approach is similar to that of Oberhuber (1993) and Large et al. (1997), we did not attempt to refine the forcing fields. Thus, the wind and air temperature fields are the same as described above. Solar radiation is calculated by astronomical and geographical parameters, similar to those in Drijfhout et al. (1996) and SKD, but without the upper constraint of 63 W m^{-2}. A cloudiness factor of 0.7 has been assumed globally. While this value is comparable to the average in mid- and high-latitudes, it is overestimated in the subtropics (e.g., Gill 1982). Nevertheless, the net radiative heat flux is overall fairly realistic, which seems partly due to the consistent usage of this cloudiness factor for the longwave (downward) back radiation. Furthermore, relative humidity has been specified to be 80% globally, which does not seem to lead to large deviations of the latent heat flux from what has been generally estimated. Overall, the spatial and seasonal patterns of the total heat flux turn out to agree reasonably well with observed climatologies (e.g., Oberhuber 1988).

3) A major change compared to SKD is the replacement of grid-cell-wide convective adjustment by subgrid-scale plume convection. The latter has been adopted from Paluszkiewicz and Romea (1997). This scheme is motivated by the observation that open-ocean convective cells tend to form on scales on the order of 1 km in convectively preconditioned areas, the latter being on the order of 100 km (e.g., Marshall and Schott 1999). While conventional convective adjustment, as used in SKD, for example, leads to grid-cell-wide overturning layer by layer in case of static instabilities, the plume parameterization is able to limit the affected area by removing grid-cell-wide instability in plumes of the observed horizontal scale. While the initial plume radius, vertical plume velocity, and plume fractional area are specified, the development of a plume is governed by the depth-dependent buoyancy flux and energy budget. Vertical displacement of unstable water parcels and subsequent entrainment-generated mixing lead to a subgrid-scale plume temperature and salinity. After penetration to a neutrally buoyant layer or the bottom, respectively, the homogeneous plume water mass becomes subject to lateral exchange with the ambient fluid in each layer that has been affected by the plume. The implementation of this scheme with a plume radius of 500 m led to overall significantly improved results, as discussed in section 1 and described in KS. While in the latter the plume parameterization has been mainly applied to the SO only, it is used globally in this study, unless otherwise noted.

4) As in KS, daily wind fields of the European Centre for Medium-Range Weather Forecasts (ECMWF) analyses are employed to drive SO sea ice dynamically as well as thermodynamically (through the turbulent heat fluxes). Instead of producing a climatology with superimposed wind variability, a year with typical SO sea-ice conditions was chosen [based on the scanning multichannel microwave radiometer (SMMR) sea ice data (Gloersen et al. 1992)], and the corresponding wind fields from the ECMWF analyses repeated annually. This forcing has been applied over all Southern Hemisphere model grid cells that contain sea ice with a mean thickness greater than 0.01 m. The daily, instead of monthly, wind variability, in particular, has been identified to play a major role by enhancing the lead fraction (e.g., Stössel 1992) and the turbulent heat flux over leads, thus enhancing sea ice formation and AABW formation (SKD).

All experiments presented in this paper are integrated to near-equilibrium according to the criteria of England (1993), that is, up to the point where the global-mean temperature and salinity in each layer change less than 0.01C° century and 0.001 psu/century, respectively. Depending on the severity of the impact per individual sensitivity experiment, this requires integrations of up to 3000 years for each experiment. All results shown are averages over the last decade of the respective experiment.

3. Results

a. Comparison to KS (experiments REF and REFCA)

Except for the heat flux forcing and the global application of the plume-convection parameterization, our

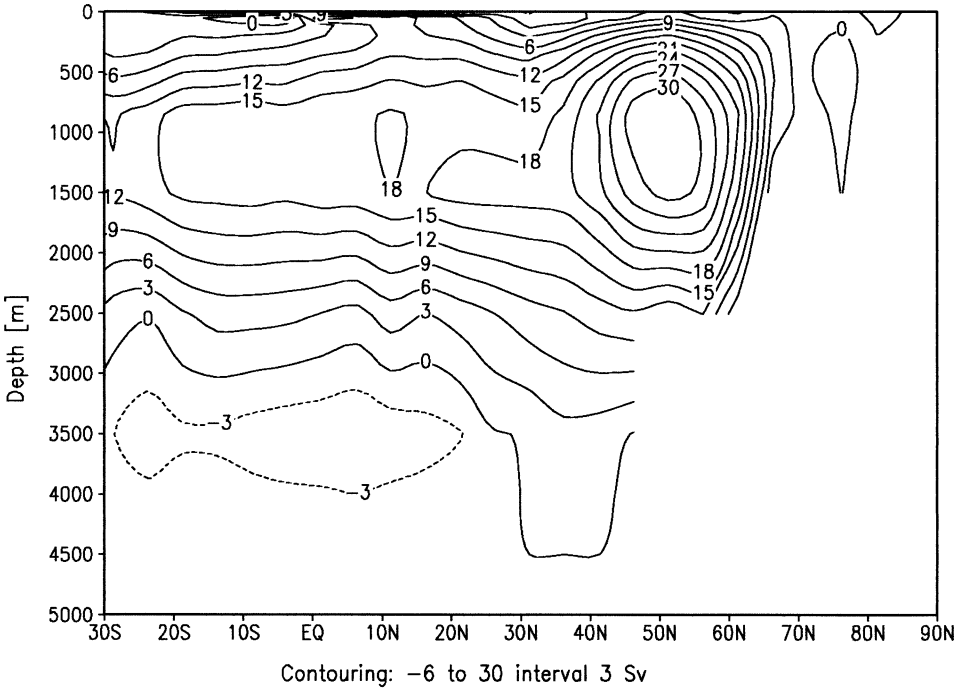

FIG. 1. Atlantic annual-mean meridional overturning streamfunction as simulated in expt REF.

reference experiment (REF) is identical to experiment MIX in KS. The most striking difference in results is a much weaker North Atlantic (NA) cell, and correspondingly since the AABW intrusion across 30°S is about the same, a weaker North Atlantic Deep Water (NADW) outflow across 30°S in the Atlantic [13 versus 16 Sv (Sv $\equiv 10^6$ m^3 s^{-1})] (Fig. 1). Here we define NADW outflow at 30°S to not include the AABW return flow, and the northward intrusion of AABW across 30°S to possibly include Circumpolar Deep Water (CDW) components (Sloyan and Rintoul 2001; A. H. Orsi 2001, personal communication). The 9 Sv weaker NA cell tends more toward observed estimates (e.g., Schmitz 1996; Ganachaud and Wunsch 2000), though it still seems substantially overestimated. The outflow of NADW, on the other hand, is in both cases within the uncertainty range of individual estimates and, in particular, within the discrepancy range between independent estimates (e.g., Sloyan and Rintoul 2001; Ganachaud and Wunsch 2000).

In terms of the global-mean deep-ocean properties, temperature increased marginally by 0.08 K compared to KS (Fig. 2), while salinity decreased substantially (with respect to its effect on deep-ocean density) by about 0.05 psu. Salinity-wise, the new results are thus overall less realistic. This is mainly due to the global application of the plume-convection parameterization, which yields weaker NADW formation and thus less of a dominance of salty NADW in global deep-ocean properties.

Upon replacement of plume convection by convective adjustment in the SO (REFCA), there is a dramatic decrease in deep-ocean temperature and salinity (Fig. 2). As observed in KS, this is commensurate with the picture that excessive open-ocean convection in the SO resulting from convective adjustment dominates the deep-ocean properties, making them too cold and too fresh.

Otherwise, the results are similar to those of KS, in particular as far as the increase of Antarctic ice thickness and the weaker Antarctic Circumpolar Current (ACC) in REF are concerned (Table 1). Implications concerning the agreement or disagreement with observed estimates was discussed in KS (and summarized in section 1). Note that although the introduction of plume convection led to major improvements, there are also deteriorations, such as the weaker ACC.

b. SO sea ice sensitivities

Three basic sea-ice-related experiments have been conducted in this study, all of which were also conducted in SKD (Table 1). The motivation for the ''salty sea ice'' (SSI) experiment is to investigate the main effect of sea ice in modifying the ocean's haline forcing, namely through the freshwater flux resulting from brine rejection during freezing and from freshwater release during melting (the effect for the ocean being similar to evaporation and precipitation). This experiment is set up such that sea ice adopts the local salinity of the upper ocean layer. This guarantees zero freshwater flux from ice freezing/melting. It does not conserve salinity when sea ice drifts into water with different surface salinity. The effect of the latter, however, is negligible compared

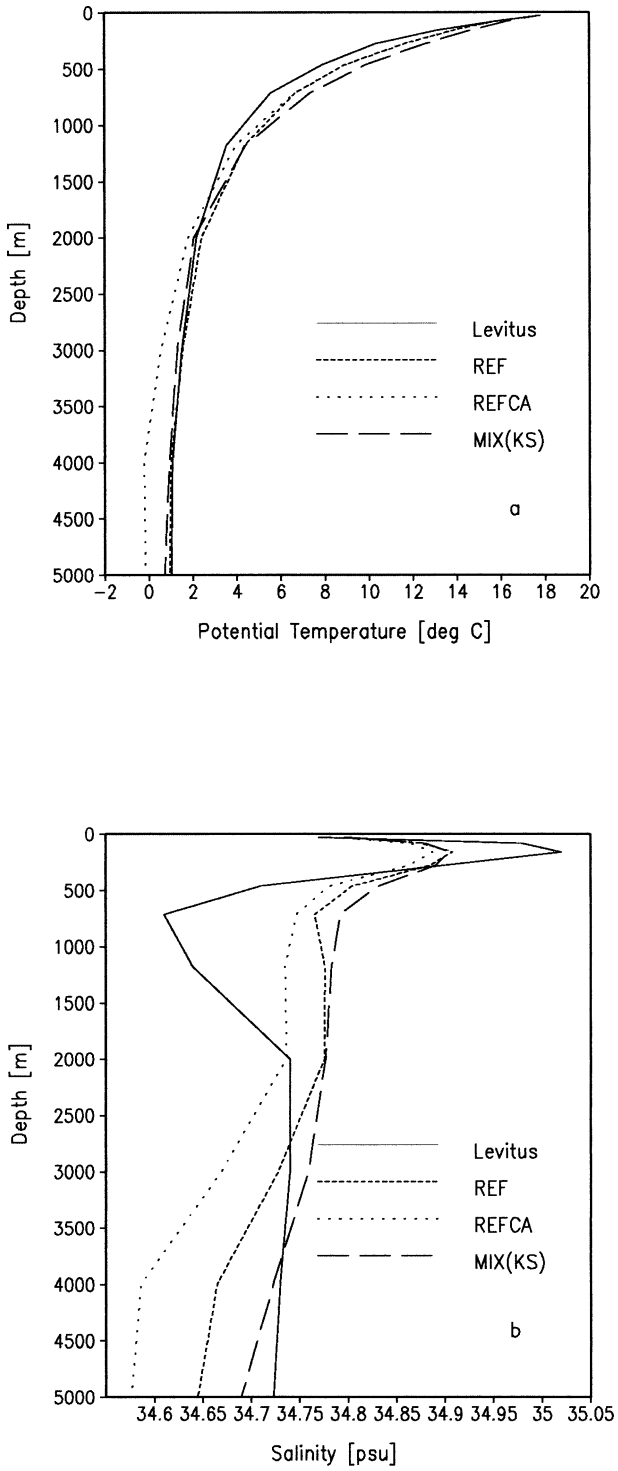

FIG. 2. Annual-mean global profiles of potential temperature (a) and salinity (b) from observations (Levitus 1982) and model experiments indicated.

to the changes introduced with this experiment (i.e., switching sea ice salinity from 5 psu to about 34 psu).

The ''dynamic sea ice forcing only by ocean currents'' (DFC) experiment is motivated by the fact that this assumption is often used in global coupled GCM simulations to force sea ice dynamically (e.g., Stouffer and Manabe 1999; Gordon et al. 2000; Levitus et al. 2001). It is based on the assumption that wind drives the upper ocean currents and that these, in turn, drive the sea ice pack. In reality, however, sea ice is directly driven by winds, mostly leading to higher ice velocity than that of the upper ocean current, the ocean thus rather acting as a retarding force on sea ice drift. The motivation for repeating this experiment here is, besides the altered convection environment, the fact that in this study the reference case is forced with winds of synoptic-scale variability rather than monthly mean winds (see section 2). Thus, while the DFC effect may be rather moderate under monthly mean winds, one may anticipate that it is enhanced under daily wind variability.

The third experiment, where a ''snow cover'' of 10 cm is assumed in areas where sea ice is thicker than 10 cm (SNC) is to investigate the insulation effect of snow [which is at least 7 times larger than that of ice (Fichefet et al. 2000)] together with its albedo effect (the snow albedo being about 1.5 times larger than that of sea ice). We intentionally did not employ the model's prognostic snow calculation, since in that case we would add precipitation in leads, and snow melt in areas where snow has been advected with sea ice. This would lead to additional effects on the buoyancy fluxes. A reasonable estimate of the latter would also require reliable precipitation data for that region (see, e.g., Marsland and Wolff 2001).

All three experiments are restricted to changes in SO sea ice and are conducted under plume convection (no suffix) as well as convective adjustment (suffix CA), see Table 1, where in the latter case plume convection is maintained in the Northern Hemisphere. We will first investigate all three sensitivities for the latter case.

1) SENSITIVITIES UNDER SO CONVECTIVE ADJUSTMENT

The reference case for this set of experiments is REFCA. The strongest impact clearly results from SSICA, with a 30% increase of NADW outflow, a 20% reduction of the Drake Passage throughflow (ACC), and a doubling of Antarctic sea ice volume (Table 1). The latter is consistent with reduced brine rejection. This reduces convection and enhances the sea ice volume since the lack of brine release stabilizes the water column, thus inhibiting the approach of oceanic heat to the surface. The resulting reduction of deep- and bottom-water formation is also consistent with a decrease of the strength of the ACC due to an overall weakening of the large-scale meridional density gradient (England 1993; Cai and Baines 1996). The associated reduction of AABW inflow into the Atlantic across 30°S by about 30% (not shown) yields a comparable percentage increase in NADW outflow. In the SSI experiment of SKD, the impact on NA overturning and NADW outflow was weaker, one reason being that in SKD sea ice had been made salty globally.

TABLE 1. Selected integral quantities from the experiments described in the text. NADW: southward flow of NADW across 30°S, ACC: Drake Passage throughflow, HANT: Antarctic sea ice volume, and OBS: observed estimates where NADW is from Macdonald and Wunsch (1996), ACC from Whitworth and Peterson (1985), and HANT from ice area according to Gloersen et al. (1992) multiplied by an estimated average thickness following Wadhams et al. (1987) and Allison et al. (2001).

Expts (sea ice related)	Convection	Acronym	NADW (Sv)	ACC (Sv)	HANT (10^3 km^3)
Observed estimates		OBS	17	130	9
Reference	Plume	REF	13.1	90.3	7.6
Salty sea ice	Plume	SSI	31.9	74.1	11.6
Dynamic forcing by currents	Plume	DFC	18.9	86.8	9.5
Snow cover	Plume	SNC	15.4	87.3	5.4
Reference	Convective adjustment	REFCA	12.1	108.3	4.2
Salty sea ice	Convective adjustment	SSICA	17.3	85.0	9.7
Dynamic forcing by currents	Convective adjustment	DFCCA	12.8	105.7	7.7
Snow cover	Convective adjustment	SNCCA	15.4	100.7	2.7
Reference	Convective adjustment reduced	REFCAR	14.7	105.0	5.7
Salty sea ice	Convective adjustment reduced	SSICAR	22.2	88.0	8.6

The global profiles (Fig. 3) reveal an overall deep-ocean warming commensurate with a reduced volume of AABW and an enhanced volume of NADW. Salinity, on the other hand, is only enhanced between 1500 and 3500 m, indicating that there is still a substantial amount of AABW formed, large chunks of which are intruded into the Atlantic (Fig. 4).

The sensitivities of DFCCA and SNCCA reveal similar tendencies as SSICA, only much weaker (Table 1), in line with SKD. Yet, the insulation and albedo effect of snow on SO sea ice (SNCCA) reveals substantial impacts, such as a warming of the deep ocean by 0.2°C, a 3 Sv increase of NADW outflow, and a weakening of the ACC by about 8 Sv. At the same time, the Antarctic sea ice volume decreased by 30%, that is, it tends in a direction opposite to that of SSICA and DFCCA. This is due to the insulation effect of snow, which normally offsets the albedo effect of snow on SO sea ice (Owens and Lemke 1990). Thus, sea ice tends to become thinner by becoming more isolated from the cold air. The combined snow–sea ice layer, however, still provides an effective insulator for the ocean. It is finally the resultant decrease in ice formation that leads to reduced brine rejection, reduced AABW formation and outflow, and ultimately a reduced ACC and enhanced NADW outflow, by the same reasoning as with SSICA.

The thicker SO sea ice in DFCCA, in contrast, is due to the upper ocean layer integrating and smoothing the daily winds, the currents of which drive the sea ice in this experiment, whereas in REFCA, the ice is directly driven by these winds. As a result, ice drift tends to be much weaker. In particular, this diminishes the momentum forcing of sea ice by katabatic winds. Thus, coastal regions that are characterized by polynyas or thin ice (i.e., potential regions for creation of HSSW) in REFCA are covered by thicker and more compact sea ice in DFCCA (not shown). Since SO convection is in all CA experiments dominated by open-ocean convection, however, the impact on AABW formation, and thus global-scale deep-ocean properties and circulation, is relatively small (as will be discussed below).

2) SENSITIVITIES UNDER PLUME CONVECTION

Table 1 reveals the major impact again occurring in SSI (relative to REF), with the tendencies generally trending in the same direction as in SSICA (relative to REFCA), but now with a much more dramatic increase of NADW outflow. As is obvious from Fig. 5 (versus Fig. 1), the NA overturning has increased considerably, the larger increase in outflow (by almost 19 Sv) compared to the increase of overturning (by about 9 Sv) being mainly related to the fact that no AABW enters the Atlantic. Correspondingly, the northward heat transport in the Atlantic increased by about 0.1 PW across all latitudes between 10°S and 40°N (not shown).

The reason for this vigorous change in the thermohaline circulation is an almost complete halt of AABW formation. This leads to a dramatic increase of deep-ocean temperature and salinity (Fig. 6), in particular in the SO (Fig. 7). This is a strikingly large impact, and we will discuss its possible meaningfulness in section 3c.

The tendencies of the other two sensitivity experiments are generally in line with the CA series in that the ACC tends to decrease, the NADW outflow to increase, and the SO ice volume to go in opposite direction. A difference now, though, is that DFC has the (much) larger impact on NADW outflow (Fig. 6). This is mainly due to the earlier mentioned reduced occurrence of coastal polynyas, the effect of which on AABW formation is now (with plume convection) not obscured by excessive open-ocean convection.

c. Discussion

In general, it can be said that the SO sea-ice-related impacts are much larger when SO convection is described by plume convection instead of convective adjustment. In this section we will focus on the reason for the strong response of SSI (versus REF) as opposed to SSICA (versus REFCA). One key element in this sensitivity study seems to be the way salty sea ice influences

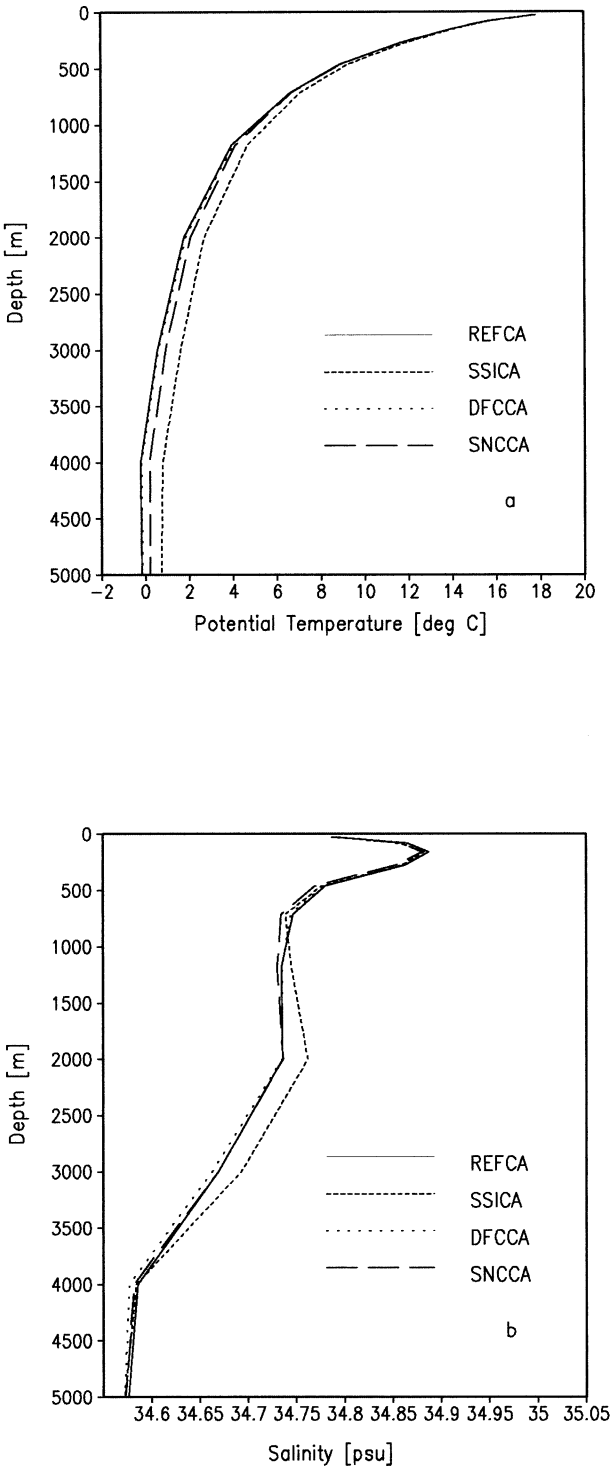

FIG. 3. Profiles of experiments as indicated; otherwise as Fig. 2.

convection in the model Weddell and Ross Seas. Concerning convective potential energy release in the Weddell Sea, the SSI sensitivities under the alternative convection schemes act in opposite direction to that of the respective reference experiments (Fig. 8).

The reason for the substantially enhanced SO convection in SSICA is a general overestimate of open-ocean convection when convective adjustment is used. This is reflected in a significantly smaller SO sea ice volume in all CA experiments and is associated with the creation of spurious open-ocean polynyas (Goosse and Fichefet 1999, 2001). In such areas of positive net annual melting, salty sea ice leads to enhanced convection, since sea ice that in the reference case is subject to melting and thus freshwater release, will in the salty sea ice case be subject to no freshwater release, thus leading to a positive feedback that enhances the already excessive convection (Fig. 8). While the effect is opposite in regions where there is no excessive convection (such as over the continental shelves), the impact on the global deep-ocean properties is overwhelmed by the process in the open-ocean polynyas. As a result, strong AABW outflow is maintained in both REFCA and SSICA.

In SSI, on the other hand, convection in the Weddell Sea has reduced to about 25% of REF (Fig. 8), which leads to an almost complete cessation of AABW formation. In REF, the latter is almost exclusively formed through near-boundary convection. In SSI (and SSICA), new-ice formation over the continental shelves is not associated with brine release, thus hindering the production of HSSW, a critical ingredient in the AABW formation process. On the other hand, in REF there is no excessive open-ocean convection that would induce and eventually trigger an acceleration of convection in the associated SSI case.

Thus, in SSICA the actual effect of neglected brine release is obscured by the reverse effect in open-ocean polynyas created by employing convective adjustment. This compensation leads to a relatively weak impact on global-scale deep-ocean properties and circulation. With plume convection in SSI, there is no such compensation, hence reflecting the ''neglected brine release'' effect more genuinely.

To establish the potentially higher credibility of the experiments that employ plume convection, we conducted a further salty sea ice experiment in which SO convection is parameterized by convective adjustment, but reduced in an ad hoc manner to every 10 days instead of every model time step (20 h). While this does not adequately mimick plume convection in the sense that convection may become locally enhanced earlier in the season (as discussed in KS), it generally reduces open-ocean convection in the SO and allows for thicker (more realistic) sea ice. This requires a new reference experiment (REFCAR, where ''R'' stands for reduced) to compare the new salty sea ice sensitivity (SSICAR) with.

The tendencies of the integrated quantities (Table 1) are similar to SSI versus REF, only much weaker. As illustrated in Fig. 9, even though SO convection is reduced in SSICAR, intrusion of AABW into the Atlantic proper is still prevalent.

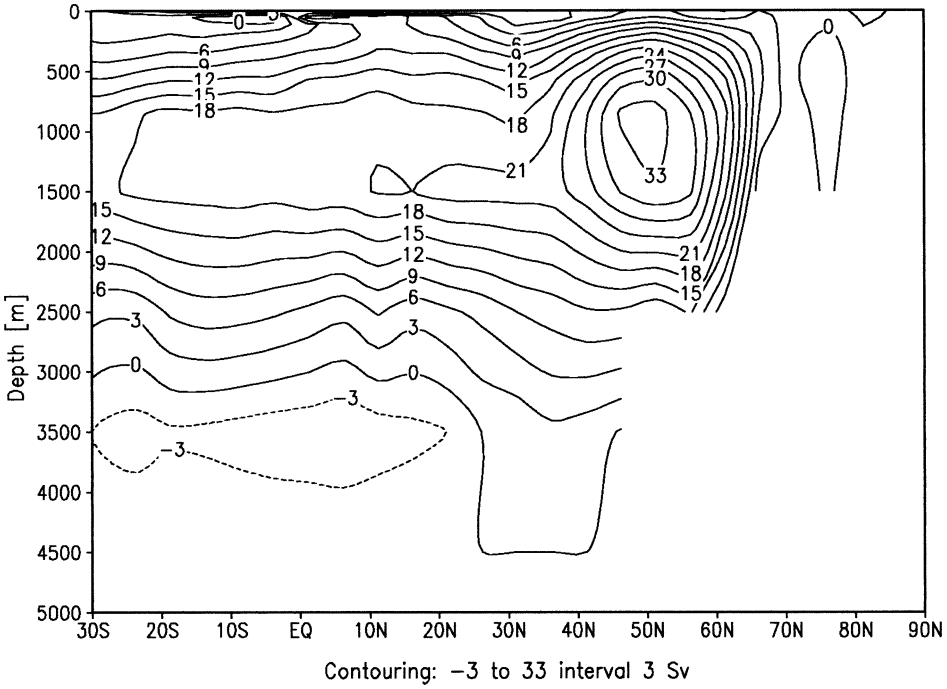

FIG. 4. Overturning streamfunction of expt SSICA; otherwise as Fig. 1.

To further analyze this issue, we compared the regional SO properties of the various SSI experiments (i.e., including CA and CAR). One such property is the abundance of HSSW, which is directly linked to the brine-release effect associated with sea ice formation over the Antarctic continental shelf, mostly in association with coastal polynyas. In view of the circumstances of the coarse model resolution, HSSW is represented quite realistically, even capturing the westward salinity enhancement over the broader shelves of the Weddell

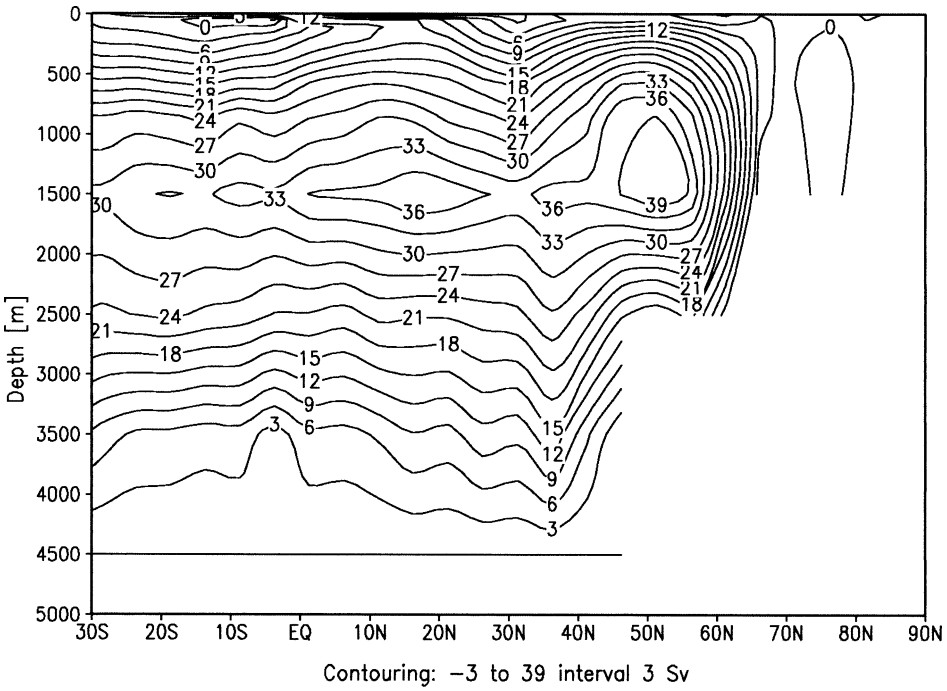

FIG. 5. Overturning streamfunction of expt SSI; otherwise as Fig. 1.

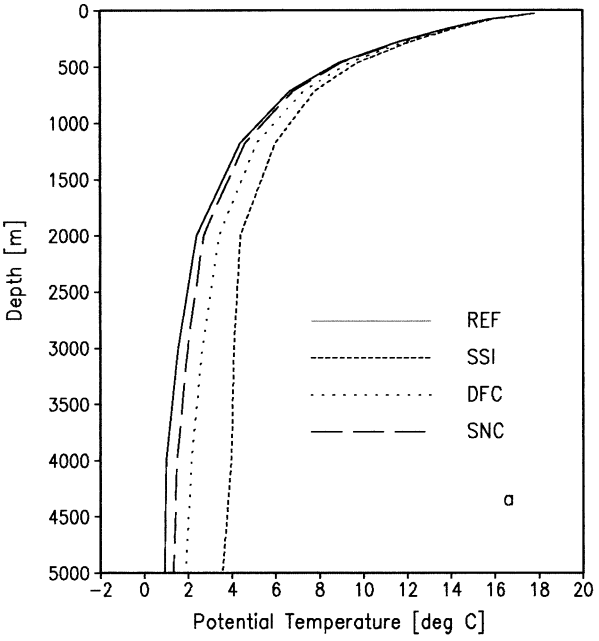

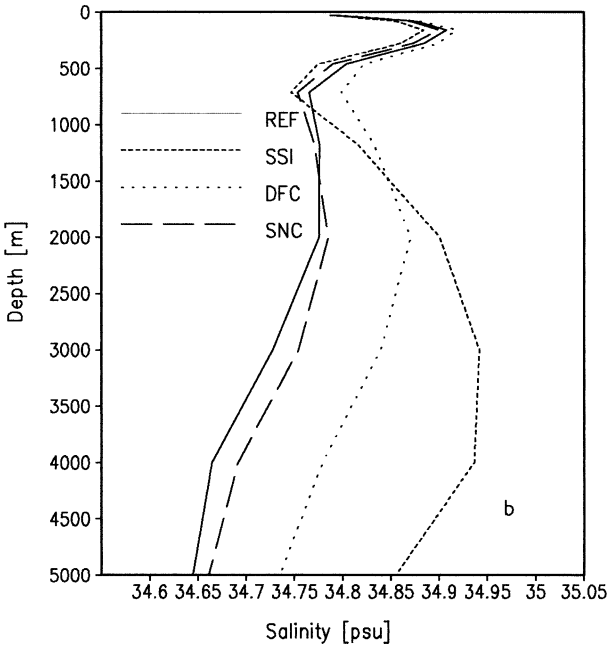

FIG. 6. Profiles of experiments as indicated; otherwise as Fig. 2.

and Ross Seas (e.g., Gill 1973; Kim and Stössel 1998). The decrease in 500 m (i.e., the deepest model shelf layer) salinity around Antarctica between the respective SSI and REF experiments being rather similar (not shown) indicates that the brine-release effect over the shelves is captured pretty much the same way in all three sets of experiments, that is, rather independently of the particular convection parameterization.

This can further be illustrated by the annual-mean convection pattern around Antarctica (Fig. 10). As is evident, convection over the shelves is significantly smaller in all SSI experiments versus the respective reference cases. Concerning open-ocean convection, however, only SSI decreases versus REF in most areas. In SSICA and SSICAR, convection is regionally significantly enhanced (versus REFCA and REFCAR, respectively) in open-ocean regions, especially in SSICA. This different behavior has a pronounced impact on deep-ocean salinities (Fig. 11). In SSI, the deep ocean is substantially saltier due to the lack of AABW. In SSICA and SSICAR, on the other hand, there are vast regions along the model deep western boundaries of the Weddell and Ross Seas that encounter a freshening associated with AABW formation via open-ocean convection. Thus, while the ad hoc reduction of convective adjustment led to several improvements over the original parameterization and revealed impacts with tendencies similar to those with the plume-convection parameterization, it still produces substantial amounts of AABW by open-ocean convection, which is not supported by modern observations.

4. Summary and conclusions

The overall intention of this study was to investigate the role of first-order SO sea-ice-related processes on global deep-ocean water mass properties and the overall thermohaline circulation. This requires several near-equilibrium sensitivity integrations; a global coarse-resolution primitive equation sea-ice–ocean GCM was thus considered the most feasible tool. A major difference in the chosen model environment compared to earlier such studies is the replacement of the commonly used grid-cell-wide convective adjustment scheme by a more comprehensive and more physical subgrid-scale plume-convection scheme. The introduction of the latter proved beneficial for capturing a number of crucial large-scale and regional features, such as the global-mean deep-ocean properties, the hydrography in the model SO, as well as SO sea ice thickness (volume) and seasonality (see KS). These improvements are all related to the removal of spurious open-ocean convection in the SO. In addition, in this study the heat flux forcing is globally determined by the surface heat balance equation (in contrast to KS and SKD). Together with plume convection being used globally, this yields a more realistic NA overturning cell than in KS, the price being a somewhat less realistic (about 0.05 psu smaller) global deep-ocean salinity. Otherwise, the reference results are similar to KS.

The particular intention of this study was to investigate three of the SO sea-ice-related sensitivities of SKD in an overall improved model environment, which

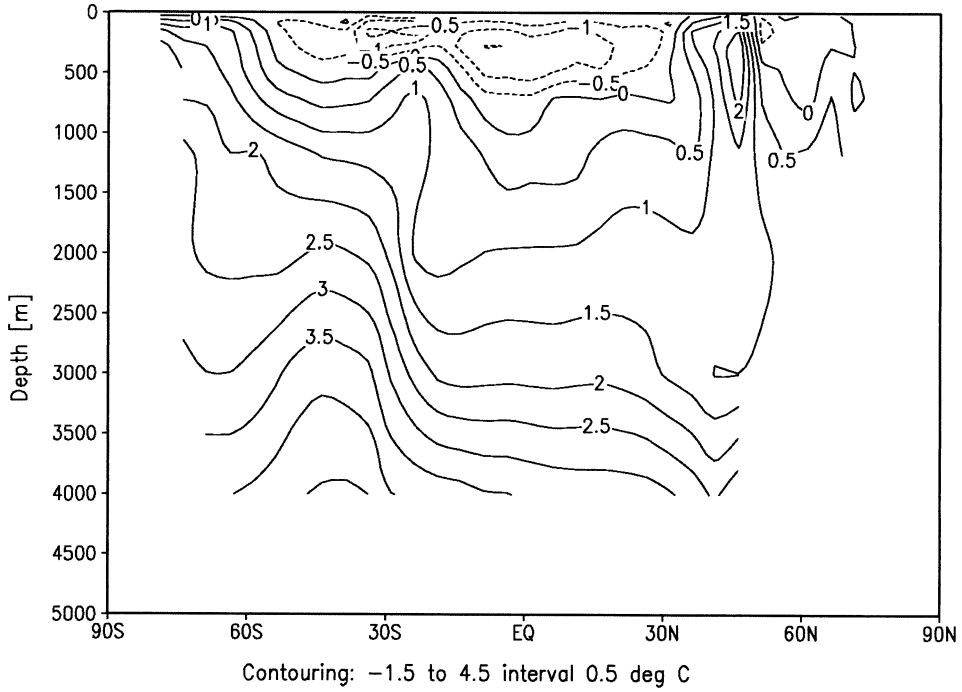

FIG. 7. Annual-mean meridional section of western Atlantic (average 60°–10°W) potential temperature difference between expts SSI and REF.

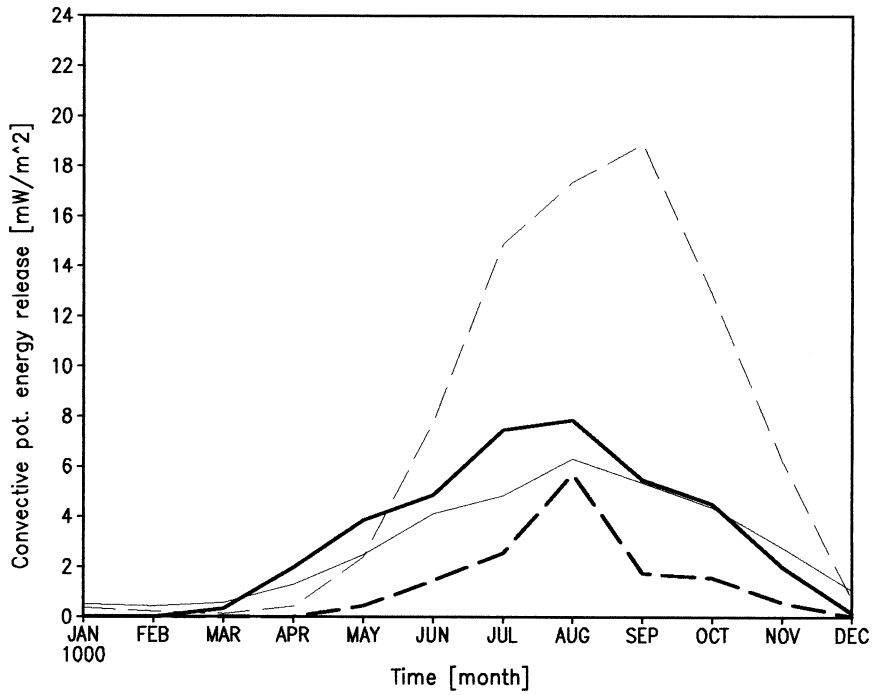

FIG. 8. Seasonal cycles of convective potential energy release in the Weddell Sea of experiments REF (thick solid line), SSI (thick dashed line), REFCA (thin solid line), and SSICA (thin dashed line).

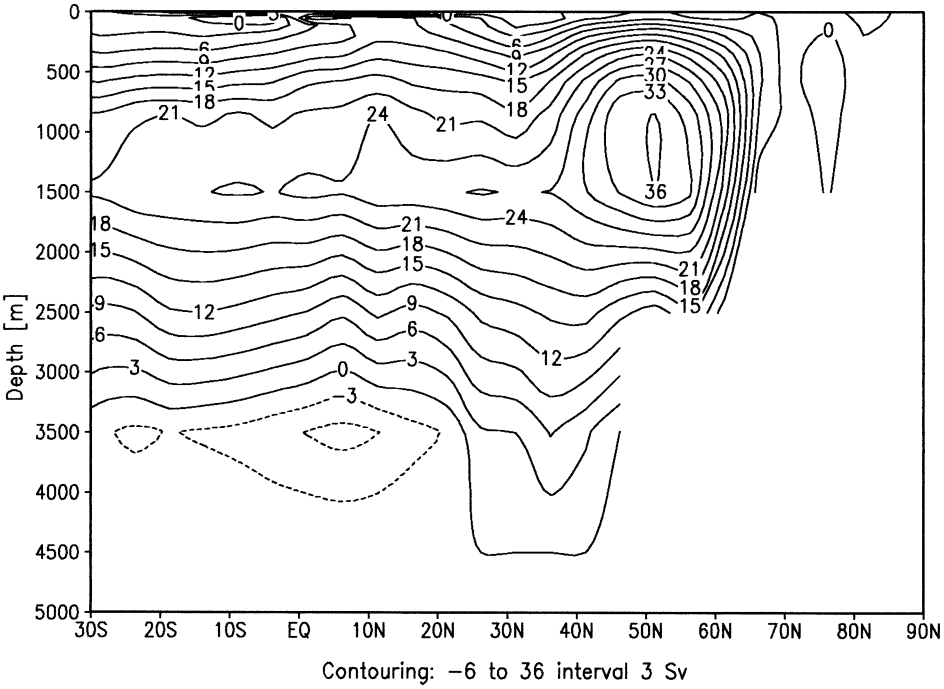

FIG. 9. Overturning streamfunction of experiment SSICAR; otherwise as in Fig. 1.

includes plume convection, daily wind forcing over SO sea ice, and realistically wide Antarctic continental shelves. By repeating the experiments under convective adjustment, we isolated the differences to be solely due to the way SO convection is treated in the model.

The effect of snow on sea ice (SNC) and of the dynamic forcing of sea ice (DFC) is generally in line with our earlier results, but consistently greater with plume convection. This is mainly due to excessive open-ocean convection in any experiment that employs convective adjustment, distorting the respective sea ice effect on deep-ocean properties (see below). In that regard, the 40% enhancement of NADW outflow and the associated substantial increase in deep-ocean temperature and salinity in DFC (versus REF) (Fig. 6) in comparison to the marginal change in DFCCA (versus REFCA) (Fig. 3) is remarkable. It indicates that a proper forcing of sea ice by winds (rather than upper-ocean currents) in the critical coastal polynyas is essential for a realistic long-term deep-ocean response. Yet, several of the most recent climate change studies with coupled atmosphere–sea ice–ocean GCMs do not consider direct wind forcing of sea ice (see section 3b).

The most striking difference from earlier simulations (e.g., Maier-Reimer 1993; SKD; Goosse and Fichefet 1999) occurred in the sensitivity experiment where sea ice was assumed to be salty (SSI). With plume convection, this experiment revealed an almost complete halt of AABW formation and a consequent dominance of NADW in the deep ocean. The reason for the occurrence of AABW formation and outflow into the world's ocean in earlier such sensitivity experiments in which convective adjustment is used is that excessive open-ocean convection masks the actual effect of neglected brine release that occurs over the continental shelves around Antarctica. In particular, regions of excessive open-ocean convection constituting regions of negative net freezing rates lead to a positive feedback in a SSI experiment by melting not being associated with freshwater release. This enhances the already excessive convection and, thus, AABW formation by open-ocean convection, thereby counteracting the effect of reduced near-boundary convection over the shelves. It ultimately renders the primary sea ice effect rather small.

As demonstrated in earlier studies (e.g., Toggweiler and Samuels 1995; Marsland and Wolff 2001; Goosse et al. 2001; Duffy et al. 1999; KS; SKD), significant changes in the rate of model AABW formation can occur due to various other processes besides a change in the way convection is treated. Such processes include the freshwater flux forcing, the variability of the wind forcing of sea ice, empirical parameters used for the sea ice component, and the parameterization of downslope flow. There are also numerous ways to parameterize convection [for an overview see Marshall and Schott (1999)]. In addition, each convection parameterization has its own set of empirical parameters.

One such parameter in the plume-convection parameterization used here (Paluszkiewicz and Romea 1997) is the initial plume radius (see section 2b). Changing it from 500 to 700 m, for example, leads to about 0.04 psu saltier global deep-ocean properties, indicating a weakening of AABW formation relative to NADW formation. A similar result is attained if plume convection

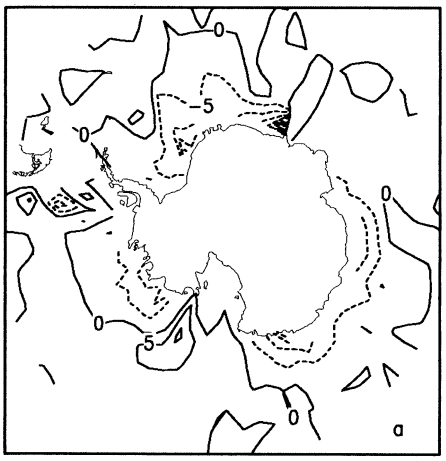

Contouring: −40 to 10 interval 5 mW/m^2

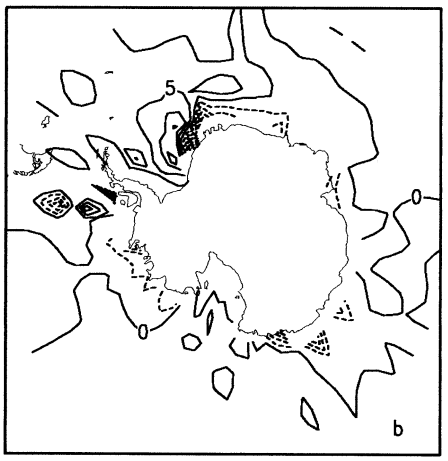

Contouring: −40 to 15 interval 5 mW/m^2

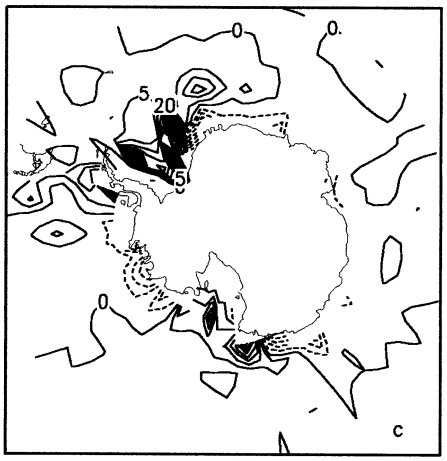

Contouring: −40 to 105 interval 5 mW/m^2

FIG. 10. Differences in annual-mean convective potential energy release of expts SSI minus REF (a), SSICAR minus REFCAR (b), and SSICA minus REFCA (c).

is replaced by convective adjustment in the Northern Hemisphere (rather than in the Southern Hemisphere, as in all CA experiments). Nevertheless, the respective associated SSI experiments yield a similar strong response as SSI versus REF, thus supporting the current results. The same is observed in corresponding experiments with a 25-layer version of the model.

Any substantial open-ocean convection in the SO being considered unrealistic under present-day climate conditions (e.g., Marshall and Schott 1999; Martinson and Iannuzzi 1998; Gordon 1998; Broecker 1999) lends further credibility to the plume-convection scheme used in this study in adding more realism to a coarse-resolution OGCM's high-latitude SO environment. Together with the earlier recognized improvements, this points toward this study delivering a more meaningful estimate of the role that SO sea ice may play in the thermohaline circulation.

Assuming that the contribution of open-ocean convection to AABW formation is indeed minimal, the discussion about the meaningfulness of our results narrows down to the question as to what extent sea ice contributes to AABW formation via near-boundary convection. In all cases presented in Figs. 10 and 11 (SSI, SSICA, and SSICAR minus their respective reference cases), there is a clear decrease of 500 m salinity over the shelves with neglected brine release. The accumulation of HSSW on the continental shelves around Antarctica is thus a decisive prerequisite for a strong global impact of SO sea ice. This is in accordance with HSSW being a crucial source water mass for the AABW formation process. If AABW is, in addition, formed by open-ocean convection, as it falsely is in most OGCMs, this critical role of HSSW tends to become obscured.

A decisive element in our approach is that we tried to capture the first-order southern high-latitude processes in concert with the global circulation. The major challenge in this attempt is to simulate the two major source waters of AABW, namely, HSSW on the Antarctic continental shelves and LCDW that borders the Antarctic continental slope. The first requires a detailed dynamic–thermodynamic sea ice model and reasonable wind fields (in particular, katabatic winds) that allow for sea ice formation and brine release in coastal polynyas, and a realistically wide model shelf topography. The second water mass can only be captured if open-ocean convection is reasonably weak, which seems difficult to achieve if grid-cell-wide convective adjustment schemes are used to remove vertical instabilities. The subgrid-scale plume-convection scheme employed in this study has ameliorated this problem significantly, rendering the current results more credible. From the present model estimate we conclude that the production of new-ice around Antarctica plays a much larger role in determining the properties and circulation of the world's deep ocean than earlier such studies have suggested.

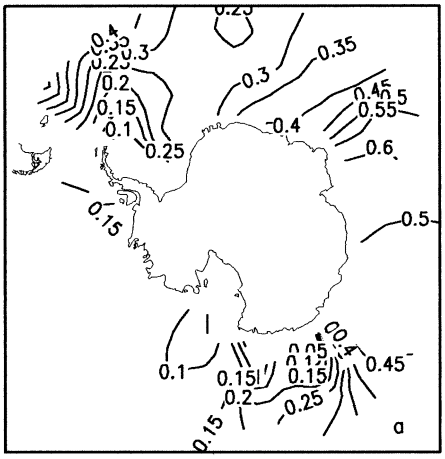

Contouring: 0 to 0.6 interval 0.05 psu

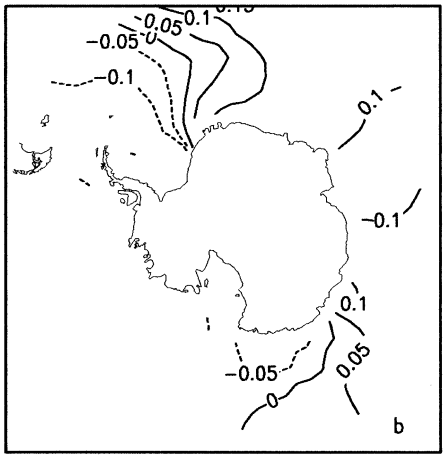

Contouring: −0.15 to 0.15 interval 0.05 psu

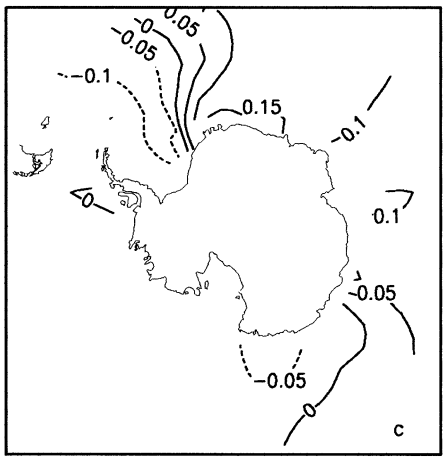

Contouring: −0.1 to 0.15 interval 0.05 psu

FIG. 11. Differences in 3000 m salinity; otherwise as in Fig. 10.

Acknowledgments. We are grateful for constructive comments received from two anonymous reviewers of this paper. Further, this paper benefitted from discussions with Philip Duffy, Hugues Goosse, Stephanie Legutke, and Alejandro Orsi (among others). Thanks are due to Terri Paluszkiewicz for providing the plume-convection model. This research was funded through NASA Grant NAG5-7751.

REFERENCES

Akitomo, K., T. Awaji, and N. Imasato, 1995: Open-ocean deep convection in the Weddell Sea: Two-dimensional numerical experiments with a nonhydrostatic model. *Deep-Sea Res.,* **42,** 53–73.

Allison, I., R. G. Barry, and B. E. Goodison, Eds., 2001: Climate and Cryosphere Project, Science and Co-ordination plan. Tech. Doc. WMO/TD-1053, WCRP-114, WMO/World Climate Research Program, Geneva, Switzerland, 76 pp.

Andreas, E. L., and B. Murphy, 1986: Bulk transfer coefficients for heat and momentum over leads and polynyas. *J. Phys. Oceanogr.,* **16,** 1875–1883.

——, and B. A. Cash, 1999: Convective heat transfer over wintertime leads and polynyas. *J. Geophys. Res.,* **104,** 25 721–25 734.

Baines, P. G., and S. Condie, 1998: Observations and modelling of Antarctic downslope flows: A review. *Ocean, Ice, and Atmosphere: Interactions at the Antarctic Continental Margin,* S. S. Jacobs and R. F. Weiss, Eds., Antarctic Research Series, Vol. 75, American Geophysical Union, 29–49.

Barnett, T. P., D. W. Pierce, and R. Schnur, 2001: Detection of anthropogenic climate change in the world's oceans. *Science,* **292,** 270–274.

Broecker, W. S., 1999: A possible 20th-century slowdown of Southern Ocean deep water formation. *Science,* **286,** 1132–1135.

Bryan, F. O., 1998: Climate drift in a multicentury integration of the NCAR Climate System Model. *J. Climate,* **11,** 1455–1471.

Cai, W., and P. G. Baines, 1996: Interactions between thermohaline- and wind-driven circulations and their relevance to the dynamics of the Antarctic Circumpolar Current, in a coarse-resolution global ocean general circulation model. *J. Geophys. Res.,* **101** (C6), 14 073–14 093.

Carmack, E. C., 1990: Large-scale physical oceanography of polar oceans. *Polar Oceanography: Part A: Physical Science,* W. O. Smith, Ed., Academic Press, 171–222.

Curry, J. A., J. L. Schramm, and E. Ebert, 1995: Sea ice–albedo climate feedback mechanism. *J. Climate,* **8,** 240–247.

Drijfhout, S. S., C. Heinze, M. Latif, and E. Maier-Reimer, 1996: Mean circulation and internal variability in an ocean primitive equation model. *J. Phys. Oceanogr.,* **26,** 559–580.

Duffy, P. B., K. Caldeira, J. Selvaggi, and M. I. Hoffert, 1997: Effects of subgrid-scale mixing parameterizations on simulated distributions of natural ^{14}C, temperature, and salinity in a three-dimensional ocean general circulation model. *J. Phys. Oceanogr.,* **27,** 498–523.

——, M. Eby, and A. J. Weaver, 1999: Effects of salt rejected during formation of sea ice on results of a global ocean–atmosphere–sea ice climate model. *Geophys. Res. Lett.,* **26,** 1739–1742.

England, M. H., 1993: Representing the global-scale water masses in ocean general circulation models. *J. Phys. Oceanogr.,* **23,** 1523–1552.

Fichefet, T., B. Tartinville, and H. Goosse, 2000: Sensitivity of the Antarctic sea ice to the thermal conductivity of snow. *Geophys. Res. Lett.,* **27,** 401–404.

Foldvik, A., T. Gammelsroed, and T. Torresen, 1985: Circulation and water masses on the southern Weddell Sea shelf. *Oceanology of the Antarctic Continental Shelf,* S. S. Jacobs, Ed., Antarctic Research Series, Vol. 43, American Geophysical Union, 5–20.

Foster, T. D., and E. C. Carmack, 1976: Frontal zone mixing and

Antarctic bottom-water formation in the southern Weddell Sea. *Deep-Sea Res.*, **23,** 301–317.
Ganachaud, A., and C. Wunsch, 2000: Improved estimates of global ocean circulation, heat transport and mixing from hydrographic data. *Nature*, **408,** 453–456.
Gill, A. E., 1973: Circulation and bottom-water production in the Weddell Sea. *Deep-Sea Res.*, **20,** 111–140.
——, 1982: *Atmosphere–Ocean Dynamics.* International Geophysics Series Vol. 30, Academic Press, 662 pp.
Gloersen, P., W. J. Campbell, D. J. Cavalieri, J. C. Comiso, C. L. Parkinson, and H. J. Zwally, 1992: Arctic and Antarctic sea ice, 1978–1987: Satellite passive microwave observations and analysis. NASA, Special Publication SP-511, 290 pp.
Goosse, H., and T. Fichefet, 1999: Importance of ice–ocean interactions for the global ocean circulation: A model study. *J. Geophys. Res.*, **104,** 23 337–23 355.
——, and ——, 2001: Open-ocean convection and polynya formation in a large-scale ice–ocean model. *Tellus*, **53A,** 94–111.
——, J.-M. Campin, and B. Tartinville, 2001: The sources of Antarctic bottom water in a global ice–ocean model. *Ocean Modelling*, **3,** 95–108.
Gordon, A. L., 1998: Western Weddell Sea thermohaline stratification. *Ocean, Ice, and Atmosphere: Interactions at the Antarctic Continental Margin*, S. S. Jacobs and R. F. Weiss, Eds., Antarctic Research Series, Vol. 75, American Geophysical Union, 215–240.
——, and B. A. Huber, 1990: Southern Ocean winter mixed layer. *J. Geophys. Res.*, **95,** 11 655–11 672.
Gordon, C., C. Cooper, C. A. Senior, H. Banks, J. M. Gregory, T. C. Johns, J. F. B. Mitchell, and R. A. Wood, 2000: The simulation of SST, sea ice extents and ocean heat transports in a version of the Hadley Centre coupled model without flux adjustments. *Climate Dyn.*, **16,** 147–168.
Grötzner, A., R. Sausen, and M. Claussen, 1996: The impact of subgrid scale sea-ice inhomogeneities on the performance of the atmospheric general circulation model ECHAM. *Climate Dyn.*, **12,** 477–496.
Harvey, L. D. D., 1996: Polar boundary layer plumes and bottom water formation: A missing element in ocean general circulation models. *J. Geophys. Res.*, **101,** 20 799–20 808.
Hellerman, S., and M. Rosenstein, 1983: Normal monthly wind stress over the world ocean with error estimates. *J. Phys. Oceanogr.*, **13,** 1093–1104.
Hibler, W. D., III, 1979: A dynamic thermodynamic sea ice model. *J. Phys. Oceanogr.*, **9,** 815–846.
Jacobs, S. S., and C. F. Giulivi, 1998: Interannual ocean and sea ice variability in the Ross Sea. *Ocean, Ice, and Atmosphere: Interactions at the Antarctic Continental Margin*, S. S. Jacobs and R. F. Weiss, Eds., Antarctic Research Series, Vol. 75, American Geophysical Union, 135–150.
——, R. G. Fairbanks, and Y. Horibe, 1985: Origin and evolution of water masses near the Antarctic continental margin: Evidence from $H_2{}^{18}O/H_2{}^{16}O$ ratios in sea water. *Oceanology of the Antarctic Continental Shelf*, S. S. Jacobs, Ed., Antarctic Research Series, Vol. 43, American Geophysical Union, 59–85.
Jiang, L., and R. W. Garwood Jr., 1995: A numerical study of three-dimensional dense bottom plumes on a Southern Ocean continental slope. *J. Geophys. Res.*, **100,** 18 471–18 488.
Khodri, M., Y. Leclainche, G. Ramstein, P. Braconnot, O. Marti, and E. Cortijo, 2001: Simulating the amplification of orbital forcing by ocean feedbacks in the last glaciation. *Nature*, **410,** 570–574.
Killworth, P. D., 1983: Deep convection in the world ocean. *Rev. Geophys. Space Phys.*, **21,** 1–26.
Kim, S.-J., and A. Stössel, 1998: On the representation of the Southern Ocean water masses in an ocean climate model. *J. Geophys. Res.*, **103,** 24 891–24 906.
——, and ——, 2001: Impact of subgrid-scale convection on global thermohaline properties and circulation. *J. Phys. Oceanogr.*, **31,** 656–674.
Large, W. G., G. Danabasoglu, S. C. Doney, and J. C. McWilliams, 1997: Sensitivity to surface forcing and boundary layer mixing in a global ocean model: Annual-mean climatology. *J. Phys. Oceanogr.*, **27,** 2418–2447.
Levitus, S., 1982: *Climatological Atlas of the World Ocean.* NOAA Prof. Paper 13, 173 pp. and 17 microfiche.
——, J. I. Antonov, J. Wang, T. L. Delworth, K. W. Dixon, and A. J. Broccoli, 2001: Anthropogenic warming of Earth's climate system. *Science*, **292,** 267–270.
Macdonald, A. M., and C. Wunsch, 1996: An estimate of global ocean circulation and heat fluxes. *Nature*, **382,** 436–439.
Maier-Reimer, E., 1993: The driving force of brine rejection on the deepwater formation in the Hamburg LSG OGCM. *Ice in the Climate System.* W. R. Peltier, Ed., NATO-ASI Series I: Global Environmental Change, Vol. 12, Springer Verlag, 211–216.
——, U. Mikolajewicz, and K. Hasselmann, 1993: Mean circulation of the Hamburg LSG OGCM and its sensitivity to the thermohaline surface forcing. *J. Phys. Oceanogr.*, **23,** 731–757.
Marshall, J., and F. Schott, 1999: Open-ocean convection: Observations, theory, and models. *Rev. Geophys.*, **37,** 1–64.
Marsland, S., and J.-O. Wolff, 2001: On the sensitivity of Southern Ocean sea ice to the surface fresh-water flux: A model study. *J. Geophys. Res.*, **106,** 2723–2741.
Martinson, D. G., 1990: Evolution of the Southern Ocean winter mixed layer and sea ice: Open ocean deepwater formation and ventilation. *J. Geophys. Res.*, **95,** 11 641–11 654.
——, and R. A. Iannuzzi, 1998: Antarctic ocean-ice interaction: Implications from ocean bulk property distributions in the Weddell Gyre. *Antarctic Sea Ice: Physical Processes, Interactions and Variability*, M. O. Jeffnes, Ed., Antarctic Research Series, Vol. 74, American Geophysical Series, 243–271.
Maykut, G. A., 1986: The surface heat and mass balance. *The Geophysics of Sea Ice.* N. Untersteiner, Ed., NATO ASI Series B: Physics, Vol. 146, Plenum, 395–464.
Oberhuber, J. M., 1988: An atlas based on the 'COADS' data set: The budgets of heat, buoyancy and turbulent kinetic energy at the surface of the global ocean. Max-Planck-Institut für Meteorologie Tech. Rep. 15, 184 pp.
——, 1993: Simulation of the Atlantic circulation with a coupled sea ice–mixed layer–isopycnal general circulation model. Part I: Model description. *J. Phys. Oceanogr.*, **23,** 808–829.
Orsi, A. H., G. C. Johnson, and J. L. Bullister, 1999: Circulation, mixing, and production of Antarctic Bottom Water. *Progress in Oceanography*, Vol. 43, Pergamon, 55–109.
Owens, W. B., and P. Lemke, 1990: Sensitivity studies with a sea ice–mixed layer–pycnocline model in the Weddell Sea. *J. Geophys. Res.*, **95,** 9527–9538.
Pacanowski, R. C., 1995: MOM 2 Documentation user's guide and reference manual. Version 1. Ocean Tech. Rep. 3, GFDL, Princeton, NJ, 561 pp.
Paluszkiewicz, T., and R. D. Romea, 1997: A one-dimensional plume model for the parameterisation of oceanic deep convection. *Dyn. Ocean Atmos.*, **26,** 95–130.
Rind, D., R. Healy, C. Parkinson, and D. Martinson, 1997: The role of sea ice in $2\times CO_2$ climate model sensitivity. Part II: Hemispheric dependencies. *Geophys. Res. Lett.*, **24,** 1491–1494.
Schmidt, G. A., and J. E. Hansen, 1999: Role of sea ice in global climate change pondered. *Eos, Trans. Amer. Geophys. Union*, **80,** p. 317.
Schmitz, W. J., Jr., 1996: On the world ocean circulation: Volume I. Tech. Rep. 96-03, WHOI, Woods Hole, MA, 140 pp.
Sloyan, B. M., and S. R. Rintoul, 2001: The Southern Ocean limb of the global deep overturning circulation. *J. Phys. Oceanogr.*, **31,** 143–173.
Stössel, A., 1992: Sensitivity of Southern Ocean sea-ice simulations to different atmospheric forcing algorithms. *Tellus*, **44A,** 395–413.
——, S.-J. Kim, and S. S. Drijfhout, 1998: The impact of Southern Ocean sea ice in a global ocean model. *J. Phys. Oceanogr.*, **28,** 1999–2018.
Stouffer, R. J., and S. Manabe, 1999: Response of a coupled ocean–

atmosphere model to increasing atmospheric carbon dioxide: Sensitivity to the rate of increase. *J. Climate*, **12,** 2224–2237.

Toggweiler, J. R., and B. Samuels, 1995: Effect of sea ice on the salinity of Antarctic bottom waters. *J. Phys. Oceanogr.*, **25,** 1980–1997.

Visbeck, M., J. Fischer, and F. Schott, 1995: Preconditioning the Greenland Sea for deep convection: Ice formation and ice drift. *J. Geophys. Res.*, **100,** 18 489–18 502.

Wadhams, P., M. A. Lange, and S. F. Ackley, 1987: The ice thickness distribution across the Atlantic sector of the Antarctic Ocean in midwinter. *J. Geophys. Res.*, **92,** 14 535–14 552.

Whitworth, T., III, and R. G. Peterson, 1985: Volume transport of the Antarctic circumpolar current from bottom pressure measurements. *J. Phys. Oceanogr.*, **15,** 810–816.

——, A. H. Orsi, S.-J. Kim, W. D. Nowlin, and R. A. Locarnini, 1998: Water masses and mixing near the Antarctic slope front. *Ocean, Ice, and Atmosphere: Interactions at the Antarctic Continental Margin*, S. S. Jacobs and R. F. Weiss, Eds., Antarctic Research Series, Vol. 75, American Geophysical Union, 1–27.

Wolff, J.-O., E. Maier-Reimer, and S. Legutke, 1997: The Hamburg Ocean Primitive Equation model HOPE. Tech. Rep. 13, Deutsches Klimarechenzentrum, Hamburg, Germany, 98 pp.

Woodruff, S. D., R. J. Slutz, R. L. Jenne, and P. M. Streurer, 1987: A comprehensive ocean–atmosphere data set. *Bull. Amer. Meteor. Soc.*, **68,** 1239–1250.